Supercond. Sci. Technol. **22** (2009) 114011 (6pp) doi:10.1088/0953-2048/22/11/114011

Bi-SQUID: a novel linearization method for dc SQUID voltage response

V K Kornev[1], I I Soloviev[1], N V Klenov[1] and O A Mukhanov[2]

[1] Physics Department, Moscow State University, Moscow 119899, Russia
[2] HYPRES, Incorporated, 175 Clearbrook Road, Elmsford, NY 10523, USA

Received 17 July 2009, in final form 31 August 2009
Published 20 October 2009
Online at stacks.iop.org/SUST/22/114011

Abstract
We show that the voltage response of a dc SQUID can be substantially linearized by the introduction of a nonlinear inductance. The inductance tuning allows us to achieve response linearity close to 120 dB. Such a nonlinear inductance can be easily formed using Josephson junction inductance. The additional junction and main inductance form a single-junction SQUID and hence the device can be called a bi-SQUID. To obtain high dynamic range commensurate to the high response linearity, one can use a serial array of nonlinear inductance dc SQUIDs. Experimental studies of a single bi-SQUID and serial arrays of bi-SQUIDs are reported and discussed.

(Some figures in this article are in colour only in the electronic version)

1. Introduction

DC SQUIDs are known and widely used as extremely sensitive amplifiers, but showing only limited linearity voltage response. In conventional low-frequency SQUID systems, improved linearity and dynamic range are obtained by using an external feedback loop which has limited bandwidth. For cases where a SQUID-based system requires a very broad bandwidth, linearization via external feedback is not feasible. A solution may be found by using Josephson junction array structures, which could provide the increase in dynamic range with number of elements N as well as highly linear voltage response due to special design of the structures [1, 2].

In this paper, we present a modified dc SQUID capable of providing highly linear voltage response. As for dynamic range, one may use a serial array of the SQUIDs to increase it up to a value comparable with the response linearity. The thermal noise voltage V_F across the serial array of N SQUIDs is proportional to the square root of N, while the voltage response amplitude $V_{max}(\Phi)$ and the transfer factor $B = \partial V/\partial\Phi$ are both proportional to N. This means that the dynamic range $D = V_{max}(\Phi)/V_F$ increases as $N^{1/2}$.

2. Bi-SQUID

We modified a conventional dc SQUID (see figure 1(*a*)) by adding a nonlinear inductive element shunting the linear inductance of the loop coupling RF magnetic flux into the SQUID. The nonlinear inductive element is a Josephson junction that remains in its superconductive state during operation (figure 1(*b*)). This nonlinear element modifies the nonlinear transfer function of the SQUID to produce a higher-linearity transfer function, thus increasing the utility of the device as a linear amplifier. The nonlinear small-signal shunt inductance is the Josephson junction inductance

$$L_J = \Phi_0\left(2\pi I_{c3}\sqrt{1-i^2}\right)^{-1} \quad (1)$$

where $i = I_{sh}/I_{c3}$ is the normalized current passing through the shunt junction. The effective loop inductance is a parallel combination of the main inductance L and the Josephson inductance L_J. The additional junction and main inductance form a single-junction SQUID. In such a way, the modified dc SQUID can be called a *bi-SQUID*. Figure 2 shows the voltage response of both the conventional dc SQUID (dashed line) and the bi-SQUID (solid line) with normalized inductance $l = 2\pi I_c L/\Phi_0 = 1$ at bias current $I_b = 2I_c$, and $I_{c3} = 1.15I_c$. This shows a triangular transfer function, where the triangle edges are quite straight. Such a device implementation makes use of a Josephson junction as a nonlinear inductive element that can largely compensate the nonlinearity associated with the conventional SQUID transfer function.

3. Voltage response linearity

The dc SQUID, modified by adding a Josephson junction shunting the loop inductance, provides extremely high

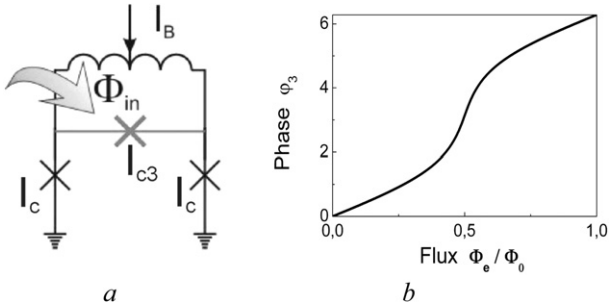

Figure 1. Bi-SQUID (*a*) and the shunt Josephson junction phase versus applied magnetic flux (*b*). Normalized inductance $l = 1$, bias current $I_b = 2I_c$, $I_{c3} = 0.85I_c$.

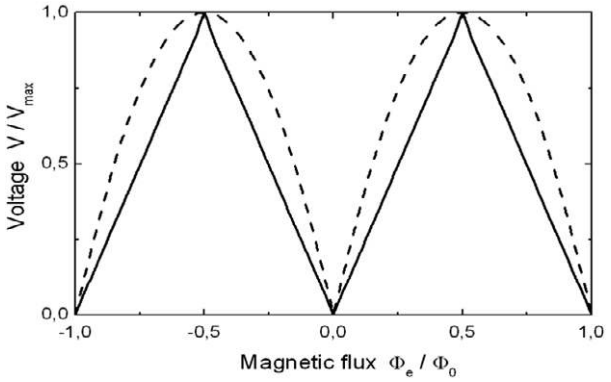

Figure 2. Voltage response of conventional dc SQUID (dashed line) and bi-SQUID (solid line) with normalized inductance $l = 1$ at bias current $I_b = 2I_c$ and $I_{c3} = 1.1I_c$.

linearity with the proper selection of parameters. This is somewhat surprising, since a Josephson junction is a nonlinear inductance. However, the junction nonlinearity is able to compensate the nonlinearity of the device in order to achieve an improved linearity close to 120 dB for significant loop inductances (which are necessary to achieve large coupling to external signals). One can note that other Josephson nonlinear reactance that functions in a similar way would have a similar effect on reducing the transfer function nonlinearity of more complex Josephson systems.

The linearity dependence on the shunt junction I_{c3} on critical current at different inductances of the bi-SQUID loop is shown in figure 3. The linearity is calculated using a single-tone sinusoidal flux input (of amplitude $A/A_{max} = 0.2$, where A_{max} corresponds to the flux amplitude $\Phi_0/4$), and measuring the total harmonic distortion in dB. This result shows that the linearity is sharply peaked for each value of l, but with different optimized values of I_{c3}. Very large values of linearity as high as ∼120 dB are achievable. Figure 4 shows how the linearity parameter varies as a function of the signal amplitude for other parameters fixed. The linearity decreases as the signal approaches the maximum value.

A serial array of bi-SQUIDs can be implemented to increase the dynamic range up to a value comparable with the response linearity. Moreover, one can build up a serial SQIF [3, 4] providing a unique voltage response with a single triangular dip at zero applied magnetic flux.

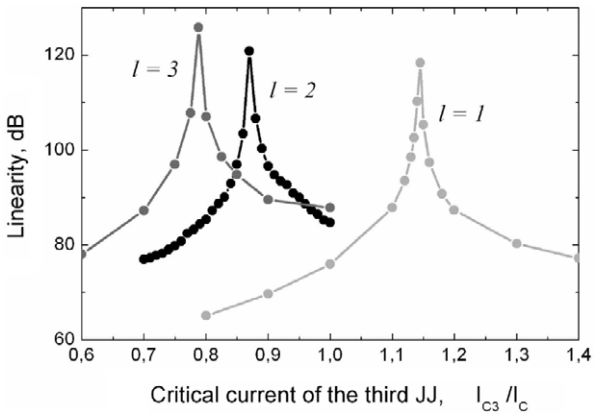

Figure 3. Dependence of the bi-SQUID voltage response linearity on critical current of the shunt junction for several fixed values of normalized loop inductance l at bias current $I_b = 2I_c$.

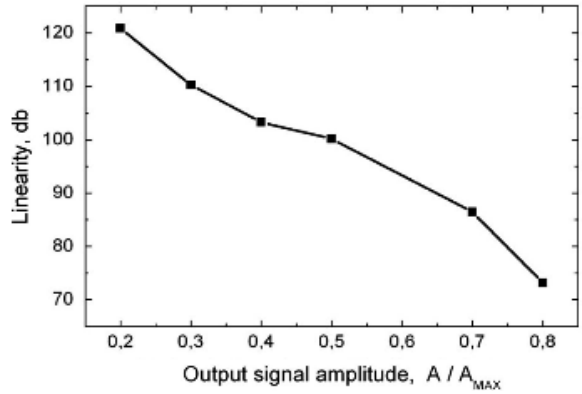

Figure 4. Dependence of the response linearity on amplitude of output signal.

4. Analytical theory

Figure 5 shows a schematic diagram of a symmetric bi-SQUID. In the frame of the RSJ model of an overdamped Josephson junction, at $I_{c1} = I_{c2} = I_c$ one can write the following simple equations in terms of standard normalized values:

$$i_b = i_1 + i_2, \qquad i_1 + i_3 = i_4, \qquad i_2 = i_3 + i_5$$

$$i_4 = \sin\varphi_1 + \dot{\varphi}_1, \qquad i_5 = \sin\varphi_2 + \dot{\varphi}_2,$$

$$i_3 = i_{c3}\sin\varphi_3 + \dot{\varphi}_3,$$

$$\varphi_1 + \frac{l}{2}i_1 = \varphi_e + \varphi_2 + \frac{l}{2}i_2,$$

$$\varphi_1 + \varphi_3 = \varphi_2, \qquad \dot{\varphi}_1 + \dot{\varphi}_3 = \dot{\varphi}_2,$$

where $i_{c3} = I_{c3}/I_c$ is the normalized critical current of the third junction, and dots denote time differentiation with normalized time $\tau = \omega_C t$, $\omega_C = \frac{2\pi}{\Phi_0}V_C$, $V_c = I_c R_N$—characteristic voltage.

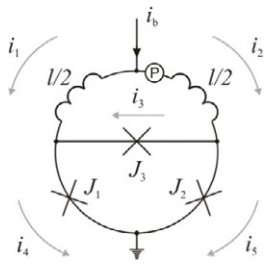

Figure 5. Schematic diagram of a bi-SQUID. 'P' is an external phase source φ_e.

The set of equations can be reduced to two equations:

$$2\dot{\varphi}_1 - \dot{\varphi}_2 = \frac{i_b}{2} + \frac{(\varphi_e + \varphi_2 - \varphi_1)}{l} + i_{c3}\sin(\varphi_2 - \varphi_1) - \sin\varphi_1 \quad (2a)$$

$$2\dot{\varphi}_2 - \dot{\varphi}_1 = \frac{i_b}{2} - \frac{(\varphi_e + \varphi_2 - \varphi_1)}{l} - i_{c3}\sin(\varphi_2 - \varphi_1) + \sin\varphi_2. \quad (2b)$$

It is more convenient to use the sum phase $\theta = \varphi_2 + \varphi_1$ and the differential phase $\psi = \varphi_2 - \varphi_1$ instead of Josephson phases φ_1 and φ_2. In this case, equations (2*a*) and (2*b*) can be rewritten as follows:

$$\dot{\theta} = i_b - 2\sin\frac{\theta}{2}\cos\frac{\psi}{2}, \quad (3)$$

$$3\dot{\psi} = -2\frac{\varphi_e + \psi}{l} - 2i_{c3}\sin\psi - 2\sin\frac{\psi}{2}\cos\frac{\theta}{2}. \quad (4)$$

In the resistive state, the sum phase θ is the running one while the differential phase ψ is a bounded function which may be represented as a sum of the slow-varying (signal) phase $\bar{\psi}$ depending on applied magnetic flux φ_e and the oscillating phase $\tilde{\psi}$. It is impossible to derive a general analytical solution of the equation set (3)–(4), but in the case of small parameter value one can use a method of successive approximations for solving equations. Such a step-by-step method was applied in [5] to analysis of a dc SQUID with a small inductive parameter $l \ll 1$.

In the case of a bi-SQUID, one can consider the oscillating phase difference $\tilde{\psi}$ as a small term. Due to the shunt junction, the term $\tilde{\psi}$ remains small at quite practical inductance parameter $l \sim 1$ (this fact is proved by numerical simulations). Therefore, we may use series distributions for θ and ψ as follows:

$$\theta = \theta_0 + \theta_1 + \ldots, \qquad \psi = \psi_0 + \psi_1 + \ldots.$$

To a first approximation corresponding to $\theta \approx \theta_0$, $\psi \approx \bar{\psi} \approx \psi_0$ when the small term $\tilde{\psi}$ is neglected, equation (3) converts to the one for a single Josephson junction with critical current value $i_c = \cos(\psi_0/2)$ under current biasing $i = i_b/2$:

$$\frac{\dot{\theta}_0}{2} = \frac{i_b}{2} - \left(\cos\frac{\psi_0}{2}\right)\sin\frac{\theta_0}{2}. \quad (5)$$

This equation has the well known analytical solution for $\theta_0(\tau)$, $\dot{\theta}_0(\tau)$ [6]; in the resistive state, time-averaging of the oscillating voltage $v(\tau) = \frac{1}{2}\dot{\theta}_0(\tau)$ results in a hyperbolic I–V curve, that in our case can be written as follows:

$$v = \frac{1}{2}\langle\dot{\theta}_0\rangle = \sqrt{\frac{i_b^2}{4} - \cos^2\left(\frac{\psi_0}{2}\right)}. \quad (6)$$

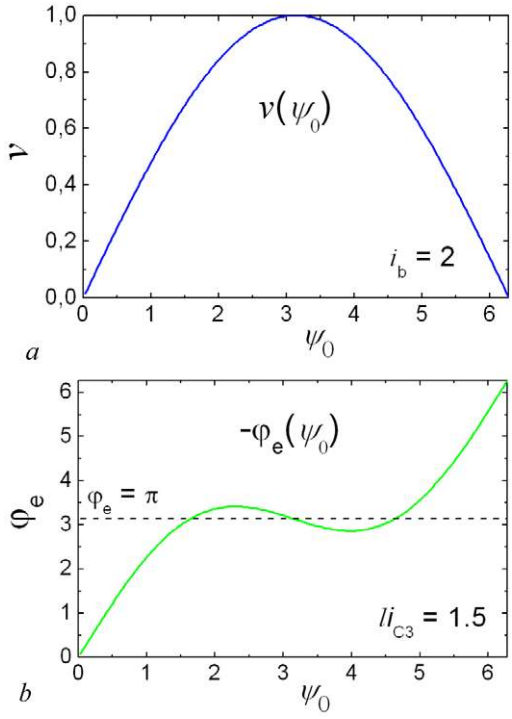

Figure 6. (*a*) Voltage dependence $v(\psi_0)$ given by equation (6) at $i_b \equiv I_b/I_c = 2$; (*b*) phase dependence $-\varphi_e(\psi_0)$ given by equation (7) at $li_{c3} \equiv 2\pi L I_{c3}/\Phi_0 = 1.5$.

Next, we do time-averaging of equation (4) and then come to the 'phase' equation

$$li_{c3}\sin(\psi_0) + \psi_0 = -\varphi_e, \quad (7)$$

because $\langle\dot{\psi}\rangle = 0$, and equation (5) determines $\langle\cos\frac{\theta_0}{2}\rangle = 0$. In fact,

$$\left\langle\cos\frac{\theta_0}{2}\right\rangle = \frac{1}{T}\int_0^{2\pi}\cos\frac{\theta_0}{2}\frac{\mathrm{d}\tau}{\mathrm{d}\theta_0}\mathrm{d}\theta_0$$
$$= \frac{1}{T}\int_0^{2\pi}\cos\frac{\theta_0}{2}\frac{\mathrm{d}\theta_0}{\left(i_b - 2\cos\left(\frac{\psi_0}{2}\right)\sin\left(\frac{\theta_0}{2}\right)\right)}$$
$$= -\frac{1}{T\cos(\psi_0/2)}\ln\left(\left|i_b - 2\cos\left(\frac{\psi_0}{2}\right)\sin\left(\frac{\theta_0}{2}\right)\right|\right)\Bigg|_0^{2\pi} = 0.$$

The first term in (7) setting a nonlinear relation between applied magnetic flux and differential phase ψ_0 is just the term responsible for linearization of the bi-SQUID transfer function $v(\varphi_e)$.

The obtained equation set (6)–(7) gives the voltage response (transfer function) of the bi-SQUID $v(\varphi_e)$ as an implicit function. One can tabulate both functional dependences $v(\psi)$ and $\varphi_e(\psi)$ and then plot the voltage response $v(\varphi_e)$. Figure 6 shows both voltage dependence $v(\psi_0)$ at $i_b \equiv I_b/I_c = 2$ and phase dependence $\varphi_e(\psi_0)$ at

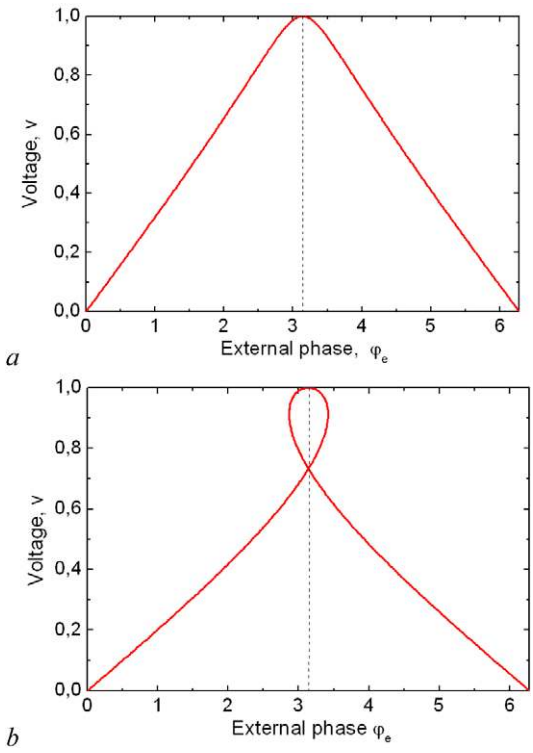

Figure 7. Voltage response $v(\varphi_e)$ given by both voltage and phase dependences $v(\psi_0)$ and $\varphi_e(\psi_0)$ at $i_b \equiv I_b/I_c = 2$ for $li_{c3} \equiv 2\pi L I_{c3}/\Phi_0 = 0.58$ (*a*) and 1.5 (*b*).

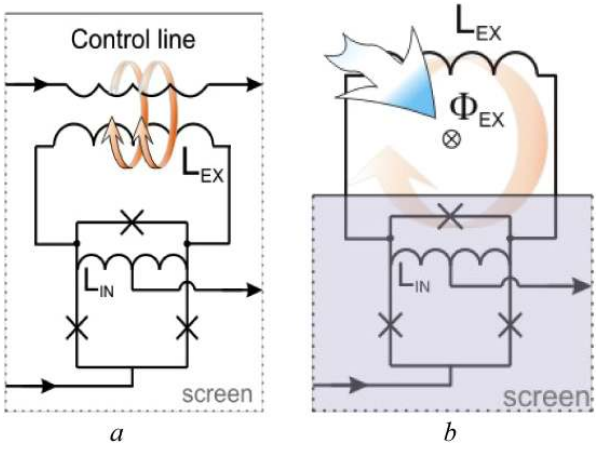

Figure 8. (*a*) Equivalent circuit of bi-SQUID with control stripline for magnetic flux application. (*b*) Equivalent circuit of the bi-SQUID cells implemented in a prototype of an active electrically small antenna.

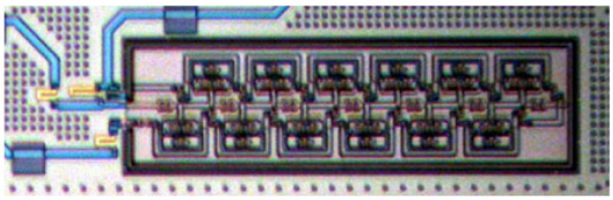

Figure 9. Microphotograph of serial array of 12 bi-SQUIDs.

$li_{c3} \equiv 2\pi L I_{c3}/\Phi_0 = 1.5$. By varying the parameter li_{c3}, one can substantially change the shape of the phase dependence. Figure 7 presents voltage response $v(\varphi_e)$ resulting from the voltage and phase dependences at different magnitudes of parameter li_{c3}. At small magnitudes of this parameter, the voltage response shape is close to the dependence $v(\psi_0)$ shown in figure 6(*a*). As the parameter li_{c3} increases, the transfer function linearity increases and the voltage response approaches a triangular shape as shown in figure 7(*a*). Further, at $li_{c3} > 1$, the phase dependence $\varphi_e(\psi_0)$ becomes a multi-valued function, and a hysteresis loop appears in the voltage response (figure 7(*b*)).

Despite the fact that the developed analytical theory is strictly valid at strong inequality $\tilde{\psi} \ll \pi/2$ and in the case of weak inequality equations (6)–(7) should be considered only as a first approximation, the obtained theoretical results are in a good agreement with the results of numerical simulations of the bi-SQUID at inductive parameter l of about 1 and even at higher values. The numerical simulations were performed using PSCAN (Personal Superconductor Circuit Analyzer) simulation software [7].

5. Experimental study

We designed, fabricated and tested a single bi-SQUID, serial arrays of bi-SQUIDs and a prototype of an active electrically small antenna based on a bi-SQUID array. Integrated circuits were fabricated using a 4.5 kA cm^{-2} Nb HYPRES process [8].

The layout design was done before the completion of numerical simulations aimed at the optimization of circuit parameters, in particular before obtaining results presented in figure 3. Therefore, the critical currents of all Josephson junctions in bi-SQUIDs were chosen to be equal ($I_{c1} = I_{c2} = I_{c3} = I_c$), while the optimal shunting junction critical current should be somewhat less for the implemented inductance parameter $l = 1.4$.

Figure 8(*a*) shows a schematic diagram of the bi-SQUID for both the fabricated single bi-SQUID and the serial array of bi-SQUIDs. To apply magnetic flux, we used a control stripline coupled magnetically with an additional transformer loop. This loop with high inductance L_{ex} is connected in parallel to inductance L_{in} and therefore practically does not change the interferometer inductance. A microphotograph of the fabricated serial array of 12 bi-SQUIDs is shown in figure 9.

Voltage response of bi-SQUID measured by automated setup OCTOPUX [9] is shown in figure 10. The applied bias current was slightly more than the critical current $2I_c$ of the bi-SQUID. The shunt junction critical current is not of the optimal value at the implemented inductance parameter. As a result, the observed voltage response is not perfectly linear, although it shows a clear triangular shape. The measured transfer function coincides closely with the one calculated using the PSCAN simulator. As for the small hysteresis at the flux value close to $\pm\Phi_0/2$, it indicates that the effective inductance parameter of a single-junction SQUID $l^* \equiv li_{c3} \equiv 2\pi L I_{c3}/\Phi_0$ is

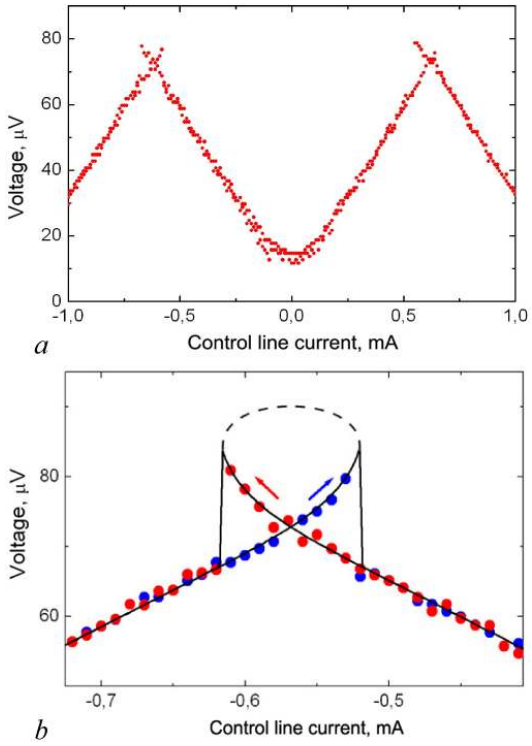

Figure 10. (*a*) Voltage response of bi-SQUID with equal critical currents of all junctions and inductive parameter $l = 1.4$. The response was measured by OCTOPUX. The applied bias current was slightly more than the SQUID critical current $2I_c$. (*b*) Top part of the measured voltage response and the fit curve (solid line) calculated using the PSCAN routine. The fitting parameters are as follows: $l = 1.4$, $l_p = 0.3$, $\beta_c = 0.2$, where β_c is the McCumber parameter, and l_p is the parasitic inductance connected in series with shunt junction. The instable part of the top loop is shown by dash line.

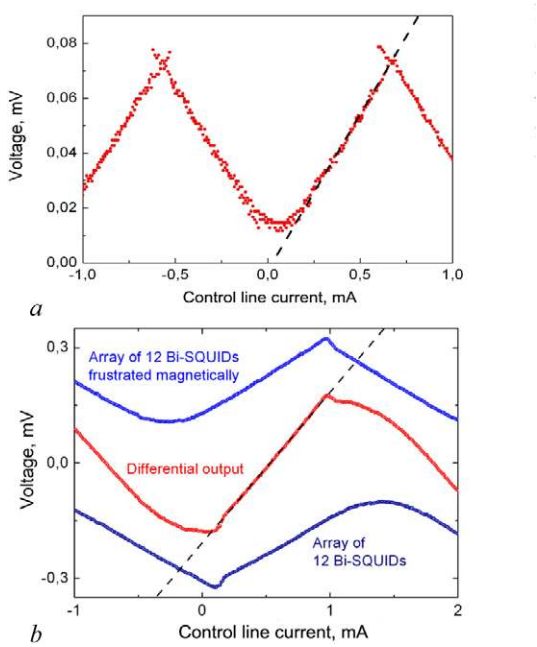

Figure 11. (*a*) Voltage response of a serial array of 12 bi-SQUIDs with equal critical currents of all Josephson junctions and inductive parameter $l = 1.4$. Hysteresis manifestations on tops of the response are smoothed due to spread in the array cell parameters and noise. (*b*) Voltage response of the differential scheme of two serial arrays of 12 bi-SQUIDs frustrated oppositely by nearly half a flux quantum as well as the source responses of the arrays biased about 10% above their critical current.

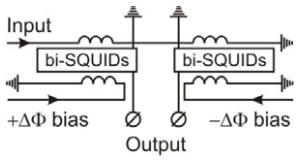

Figure 12. The differential connection of bi-SQUIDs or bi-SQUID serial arrays oppositely frustrated can be used for additional improvement of voltage response linearity.

more than unity and hence the static phase diagram becomes hysteretic. Figure 10(*b*) shows the top part of the measured voltage response and the fit curve (solid line) calculated using PSCAN. The fitting parameters are as follows: $l = 1.4$, $l_p = 0.3$, $\beta_c = 0.2$, where β_c is the McCumber parameter and l_p is the parasitic inductance connected in series with a shunt junction. The dashed line shows an instable part of the hysteretic loop.

The voltage response of the array measured by OCTOPUX is presented in figure 11(*a*). The applied bias current was slightly more than the critical current of the array. The hysteresis manifestations on top sections of the voltage response are smoothed due to spread in the array cell parameters and noise. The voltage response linearity of both the bi-SQUID and the bi-SQUID serial array can be additionally improved by means of differential connection of two identical bi-SQUIDs or serial arrays oppositely frustrated (figure 12). This improvement results from cancellation of even harmonics of the individual responses. Figure 11(*b*) shows the voltage response of the differential scheme of two serial arrays of 12 bi-SQUIDs frustrated by nearly half a flux quantum. The arrays are biased at about 10% above their critical currents. The increase in the bias current decreases both the array response amplitude and the response linearity. Despite this fact, the differential response shows a good linearity within a substantially wide range.

Figure 13 shows a microphotograph of the fabricated prototype of an active electrically small antenna based on a serial array of 12 bi-SQUIDs. Each bi-SQUID is equipped with a large superconducting loop (see the equivalent scheme of such a bi-SQUID in figure 8(*b*)) to sense the magnetic component B of an incident electromagnetic wave. To perform an initial test of such an antenna, a large-size strip coil was integrated on the fabricated chip to excite a low-frequency or dc magnetic field. Figure 14 shows the voltage response of the antenna prototype with 50 Ω load. The applied bias current is slightly more than the critical current of the circuit. The antenna voltage response to a spatial magnetic field is just the same as the one observed for array of bi-SQUIDs with a control current strip line. This fact confirms the validity of our design.

The performance of such an antenna can be substantially increased by combining with a flux concentrator.

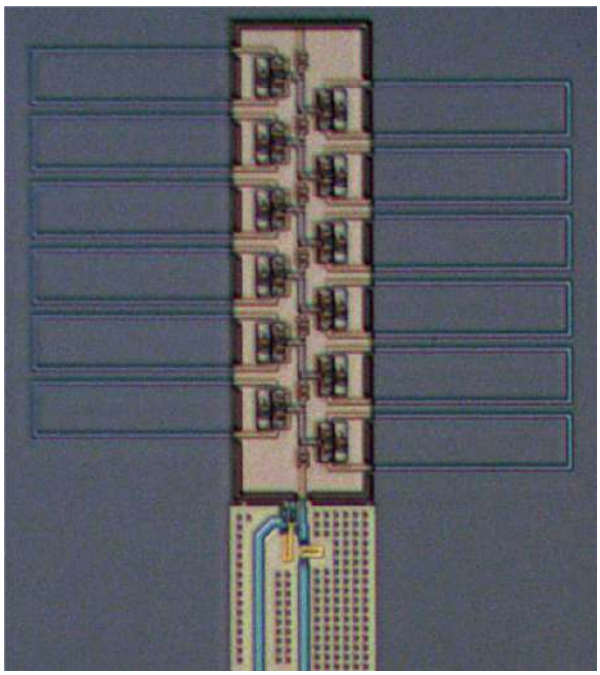

Figure 13. Microphotograph of the fabricated prototype of an active electrically small antenna based on a serial array of 12 bi-SQUIDs each equipped with a large superconducting loop to sense the magnetic component B of an incident electromagnetic wave. A large-size strip coil is introduced in the chip to excite a low-frequency or dc magnetic field.

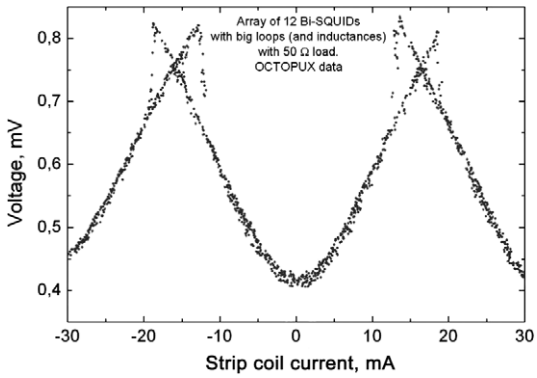

Figure 14. Voltage response of the antenna prototype with a 50 Ω load. The graph is shown versus the strip coil control current exciting low-frequency magnetic field.

6. Conclusion

We have proposed a so-called *bi-SQUID* in order to achieve a highly linear voltage response with linearity parameter as high as 120 dB for significant loop inductance allowing large coupling to external signals. The device exploits a Josephson junction as a nonlinear inductive element, which can largely compensate the nonlinearity of the conventional SQUID transfer function.

Theoretically, one can increase the dynamic range by using a serial array of such SQUID elements and determining the number of elements by balancing the required signal amplitude with the required amplifier linearity.

One should note the peak-like dependence of the linearity parameter on the shunt junction critical current. This indicates certain limitations of allowable technological spread in Josephson junction parameters for practical implementations of a highly linear serial array of bi-SQUIDs.

We designed, fabricated and tested a single bi-SQUID, serial arrays of bi-SQUIDs and a prototype of an active electrically small antenna based on a bi-SQUID array. The obtained experimental data are in good correspondence with results of numerical simulations and can be qualitatively described with the analytical theory developed.

Acknowledgments

This work was supported in part by the ONR via CRDF grant RUP1-1493-MO-05 and Russian Grants for Scientific Schools 5408.2008.2 and 133.2008.2.

The authors thank Michael Yu Kupriyanov for fruitful discussions of the theoretical study presented as well as Alex Kirichenko and Henrik Engseth of HYPRES for help in layout design verification and testing.

References

[1] Kornev V K, Soloviev I I, Klenov N V and Mukhanov O A 2009 High linearity SQIF-like Josephson-junction structures *IEEE Trans. Appl. Supercond.* **19** 741–4

[2] Kornev V K, Soloviev I I, Klenov N V and Mukhanov O A 2009 Dynamic range and high linearity issues in multi-element Josephson structures *Int. Supercond. Electronics Conf. (Fukuoka, June)* HF-P03 Ext. Abstracts

[3] Haeussler Ch, Oppenlaender J and Schopohl N 2001 Nonperiodic flux to voltage conversion of series arrays of dc superconducting quantum interference devices *J. Appl. Phys.* **89** 1875

[4] Oppenlaender J, Häussler Ch, Traeuble T and Schopohl N 2002 Sigmoid like flux to voltage transfer function of superconducting quantum interference filter circuits *Physica* C **368** 125

[5] De Luca R, Fedullo A and Gasanenko G 2007 Pertubation analysis of the dynamical behavior of two-junction interferometers *Eur. Phys. J.* B **58** 461–7

[6] Likharev K K 1986 *Dynamics of Josephson Junctions and Circuits* (New York: Gordon and Breach) p 634

[7] Kornev V K and Arzumanov A V 1997 Numerical simulation of Josephson-junction system dynamics in the presence of thermal noise *Inst. Physics Conf. Ser. No 158* (Bristol: Institute of Physics Publishing) pp 627–30

[8] Available online at http://www.hypres.com/

[9] Available online at http://gamayun.physics.sunysb.edu/RSFQ/Research/octopus.html